THE JOURNAL OF BIOLOGICAL CHEMISTRY
Vol. 278, No. 17, Issue of April 25, pp. 15313–15318, 2003
Printed in U.S.A.

A Broken α-Helix in Folded α-Synuclein*

Received for publication, December 23, 2002, and in revised form, February 11, 2003
Published, JBC Papers in Press, February 13, 2003, DOI 10.1074/jbc.M213128200

Sreeganga Chandra‡§¶, Xiaocheng Chen‖, Josep Rizo‖, Reinhard Jahn§, and Thomas C. Südhof‡¶‖

From the ‡Center for Basic Neuroscience, Department of Molecular Genetics, and Howard Hughes Medical Institute, and the ‖Departments of Biochemistry and Pharmacology, University of Texas Southwestern Medical Center, Dallas, Texas 75390-9111, and the §Max-Planck-Institut für Biophysikalische Chemie, 37075 Göttingen, Germany

α-Synuclein is a small cytosolic protein of presynaptic nerve terminals composed of seven 11-residue repeats and a hydrophilic tail. α-Synuclein misfolding and dysfunction may contribute to the pathogenesis of Parkinson's disease and neurodegenerative dementias, but its normal folding and function are unknown. In solution, α-synuclein is natively unstructured but assumes an α-helical conformation upon binding to phospholipid membranes. We now show that this conformation of α-synuclein consists of two α-helical regions that are interrupted by a short break. The structural organization of the α-helices of α-synuclein was not anticipated by sequence analyses and may be important for its pathogenic role.

In recent years, the presynaptic protein α-synuclein has attracted much attention because of its involvement in neurodegenerative diseases (1–3). Two independent mutations in human α-synuclein cause familial Parkinson's disease, and wild type α-synuclein is a major component of Lewy bodies, cytoplasmic inclusion bodies found in Parkinson's disease and in several forms of neurodegenerative dementia. However, independent of its role in neurodegenerative diseases, α-synuclein is an interesting protein in its own right. It is an abundant presynaptic protein that may regulate neurotransmitter release and may contribute to synaptic plasticity (4–6). α-Synuclein is the founding member of a protein family that additionally includes β- and γ-synucleins and synoretin (7–9). The sequences of all synucleins are similar, although only α-synuclein is implicated in disease. Synucleins are composed of six copies (β-synuclein) or seven copies (all other synucleins) of an unusual 11-residue imperfect repeat, followed by a variable short hydrophilic tail. Synucleins are soluble, natively unfolded proteins that avidly bind to negatively charged phospholipid membranes and become α-helical upon binding (10). Although secondary structure predictions indicate that the synuclein repeats could form an amphipathic structure consistent with lipid binding, the α-helical conformation is puzzling because the synuclein repeats are punctuated by central glycine residues. Furthermore, in Lewy bodies α-synuclein is thought to be in a β-strand aggregate, but aggregation of α-synuclein into dimers and multimers is promoted by lipid environments that induce an α-helical conformation (11–13). In the present study, we have examined the conformation of α-synuclein in lipidic environments to understand the relation of its sequence to its physicochemical properties and to map a potential pathway of misfolding in neurodegenerative disease.

EXPERIMENTAL PROCEDURES

Production of α-Synuclein—Recombinant α-synuclein was expressed in bacteria as GST-fusion proteins with a TEV protease recognition sequence preceding the N-terminal methionine and cleaved with TEV protease (Invitrogen), resulting in a single additional glycine residue at the N terminus. After TEV cleavage, α-synuclein was isolated as the only heat-stable component upon boiling for 15 min, purified by ion-exchange chromatography on a MonoQ column (Amersham Biosciences), and dialyzed against the appropriate experimental buffers. N^{15} and C^{13}/N^{15} double-labeled α-synuclein were prepared similarly from bacteria grown in minimal M9 media supplemented with $N^{15}H_4Cl$ and C^{13}D-Glucose (Cambridge Isotope Laboratories).

Antibodies—Antibodies were raised in rabbits against a peptide corresponding to amino acid 2–24 of human α-synuclein (CDVFMKGLSKAKEGVVAAAEKTKQG) that was coupled via its N-terminal cysteine to keyhole limpet hemocyanin, and against recombinant α-synuclein expressed in bacteria.

Partial Tryptic Digestion—α-Synuclein (13.8 μM) was incubated for the indicated times at room temperature in the presence of SUVs[1] (280 molar excess; composition: 30% phosphatidylserine/70% phosphatidylcholine or 100% phosphatidylcholine) or SDS (1 mM) in 20 mM Tris-HCl, pH 7.4, with 0.2% (SUVs) or 2% (SDS) trypsin (Sigma). Digestion products were separated on 16.5% Tris-Tricine gels (14) and analyzed by Coomassie Blue staining or immunoblotting.

NMR Spectroscopy—NMR data were acquired at 25 °C on Varian INOVA500 or INOVA600 NMR spectrometers. All NMR experiments were performed with pulsed-field gradient enhanced pulse sequences (15, 16) using H_2O/D_2O 95:5 as the solvent. Sample conditions for ^1H-^{15}N HSQC spectra are indicated in the corresponding figure legends. Backbone assignments were obtained from three-dimensional ^1H-^{15}N NOESY-HSQC, TOCSY-HSQC, HNCO, HNCACB, and CBCA(CO)NH experiments acquired on a 0.3 mM sample of α-synuclein dissolved in 20 mM phosphate buffer, pH 7.4, plus 50 mM SDS. The 3D ^1H-^{15}N NOESY-HSQC data were also used to analyze secondary structure NOE patterns and search for long-range NOEs.

Miscellaneous—SUVs of 100% brain phosphatidylcholine or 30% brain phosphatidylserine, 70% brain phosphatidylcholine (all from Avanti Polar Lipids) were made and quantified as described (17). SUVs were confirmed to be unilamellar by electron microscopy. SDS-PAGE and immunoblotting were performed using standard procedures. CD spectra were recorded at 25 °C in a Jasco Model J-720 instrument upgraded to J-715U and equipped with a 6-position peltier cuvette holder. Recordings were made using Hellma Quartz cuvettes (path length 0.1 cm). Spectra were averaged from 10–50 scans of 0.2 nm steps at a rate of 50 nm/min. Edman degradation was carried out using standard procedures.

* This study was supported by grants from the National Institutes of Health (1-RO1-NS40057) (to T. C. S.) and the Deutsche Forschungsgemeinschaft (Gottfried-Wilhelm Leibnitz program) (to R. J.). The costs of publication of this article were defrayed in part by the payment of page charges. This article must therefore be hereby marked "*advertisement*" in accordance with 18 U.S.C. Section 1734 solely to indicate this fact.

¶ To whom correspondence may be addressed. Tel.: 214-648-1876; Fax: 214-648-1879; E-mail: Thomas.Sudhof@UTSouthwestern.edu (to T. S.); or E-mail: Sreeganga.Chandra@UTSouthwestern.edu (to S. C.).

[1] The abbreviations used are: SUV, small unilamellar vesicle; CD, circular dichroism; HSQC, heteronuclear single quantum correlation; NMR, nuclear magnetic resonance; NOE, nuclear Overhäuser effect; NOESY, nuclear Overhäuser Effect Spectroscopy; TOCSY, total correlation spectroscopy.

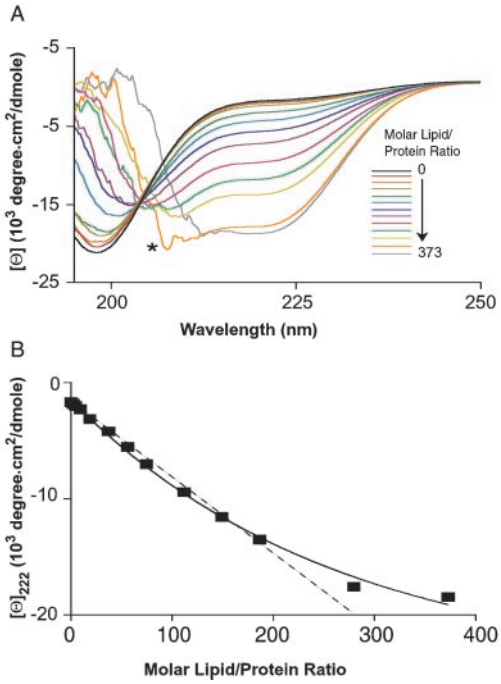

FIG. 1. **Titration of α-synuclein folding with negatively charged phospholipid vesicles.** *A*, circular dichroism spectra of α-synuclein (13.8 μM) mixed with increasing amounts of SUVs (composition: 30% brain phosphatidylserine, 70% phosphatidylcholine; *asterisk*, scattering artifact at high liposome concentrations). No changes were observed with pure phosphatidylcholine SUVs (not shown). *B*, plot of the molar ellipticity of α-synuclein at 222 nm as a function of the molar lipid/protein ratio. Note that folding saturates at ~270–300 phospholipid molecules per α-synuclein molecule. Similar results were obtained in three separate experiments.

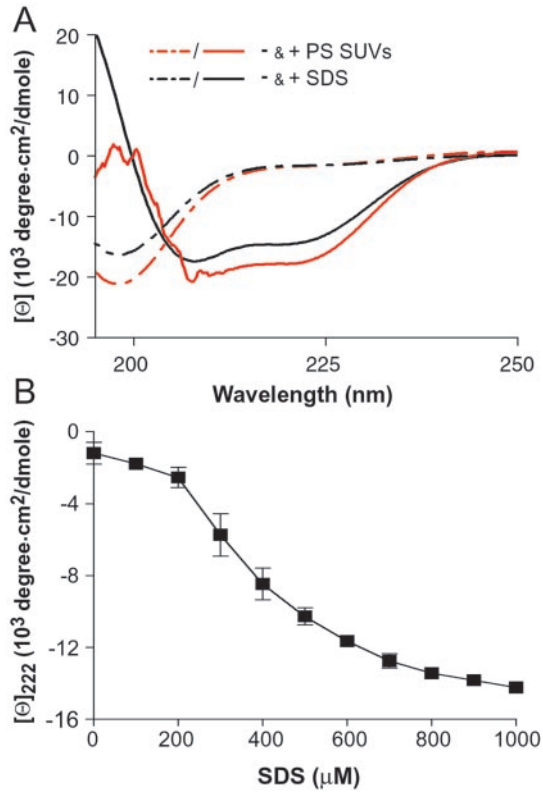

FIG. 2. **Folding of α-synuclein promoted by detergents.** *A*, circular dichroism spectra of α-synuclein in the presence of SUVs containing phosphatidylserine or of SDS (13.8 μM α-synuclein was mixed with SUVs added at a molar lipid to protein ratio of 280:1 or 1 mM SDS). *B*, molar ellipticity of α-synuclein (13.8 μM) at 222 nm as a function of SDS concentration (data shown are means ± S.E. of three independent experiments).

RESULTS AND DISCUSSION

Phospholipid-induced Folding of α-Synuclein—Upon addition of SUVs containing 30% phosphatidylserine and 70% phosphatidylcholine, the CD spectrum of purified α-synuclein shifts from a characteristic random coil pattern with a 195 nm minimum to a typical α-helical pattern with 206 and 222 nm minima (Fig. 1*A*) (10). Thus phosphatidylserine-containing SUVs induce α-synuclein folding ("folding" as used here refers to the adoption of a secondary, but not necessarily tertiary structure). SUVs composed only of phosphatidylcholine caused little change (data not shown). To determine how many lipids are required for α-synuclein folding, we titrated α-synuclein with increasing amounts of SUVs with a precisely known phospholipid content that were confirmed by electron microscopy to be unilammellar. A progressive increase in α-synuclein folding was observed, with apparent saturation of folding at a molar lipid/protein ratio of ~270–300:1 (Fig. 1*B*). Taking into account that SUVs are composed of phospholipid bilayers, this ratio indicates that binding of each synuclein molecule requires ~140–150 phospholipid molecules.

Detergent-induced α-Synuclein Folding—To examine the conformation of folded α-synuclein, it is necessary to achieve folding in solution. Therefore we used CD spectroscopy to examine a series of detergents for their ability to support α-synuclein folding. Most detergents tested (Nonidet P-40, *n*-octylglycoside, Thesit, Tween 20, 3-[(3-cholamidopropyl)dimethylammonio]-1-propanesulfonic acid, cholic acid, deoxycholic acid, and taurocholic acid) did not induce folding (data not shown). Only lysosphatidylserine, lysophosphatidic acid (but not lysophosphatidylcholine), and SDS elicited the same CD change in α-synuclein as acidic SUVs (Fig. 2*A* and data not shown).

Because complexes of α-synuclein with SDS would be particularly useful in characterizing its structure, we tested whether small phospholipid vesicles and SDS induced similar folded states of α-synuclein. Titration of α-synuclein with increasing concentrations of SDS revealed that SDS promotes folding below its critical micellar concentration (7–10 mM), with complete folding at 1 mM SDS for 13.8 μM α-synuclein (Fig. 2*B*). This result suggests that ~70 SDS molecules are required per α-synuclein molecule for complete folding, a number that approximates the aggregation number for SDS (*i.e.* the number of SDS molecules per micelle) (18). Thus it is possible that α-synuclein drives the formation of SDS micelles and folds, as in the case of SUVs, on the surface of the micelles.

Folding Results in Partial Protection from Proteolysis—Limited tryptic digestion of α-synuclein revealed that in the presence of saturating concentrations of SUVs containing phosphatidylserine, α-synuclein was partly protected from proteolysis, whereas SUVs lacking phosphatidylserine had no effect (Fig. 3). Similarly, when we added 1 mM SDS, we also observed partial protection from proteolysis, although the precise pattern of protected fragments was different, presumably because SDS affected the digestion. Immunoblotting with site-specific antibodies showed that the protected fragments (~6 kDa, ~4 kDa) under both conditions were derived from the N-terminal region of α-synuclein (Fig. 3). We were unable to ascertain the mass of these fragments by matrix-assisted laser desorption ionization time-of-flight experiments due to lipidic contaminants, but analysis by Edman degradation confirmed that the 4–6 kDa fragments correspond to the N terminus of α-synuclein. Judging from their size, we surmised that one of the cleavage sites is probably at lysines 43 or 45. In support of this conclusion, tryptic digestion of mutant α-synuclein that

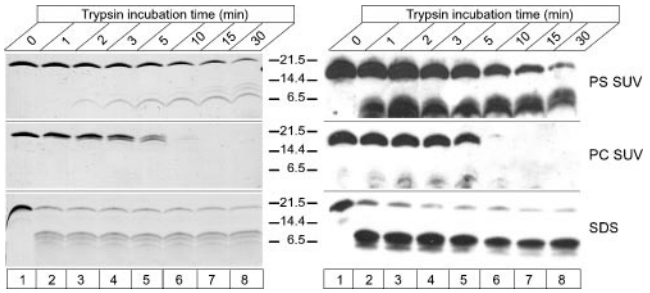

FIG. 3. **Partial tryptic digestion of α-synuclein.** Digestion of α-synuclein (40 μg) by trypsin in the presence of SUVs composed of only phosphatidylcholine (*PC SUV*) or of 30% phosphatidylserine, 70% phosphatidylcholine (*PS SUV*, both vesicles were added at a molar lipid to protein ratio of 280:1), or in the presence of SDS (1 mM). Digests were stopped at the indicated times, and proteins were analyzed on Tris-Tricine gels stained with Coomassie Blue (*left panels*). Edman degradation and parallel immunoblotting with an antibody to the N-terminal 24 residues of α-synuclein demonstrated that the protected fragments in the PS SUV and SDS samples were derived from the N terminus of α-synuclein (*right panels*). *Numbers between* the *panels* denote migration of molecular weight markers.

lacks these lysines did not produce 4–6 kDa protected fragments (data not shown).

NMR Analysis of Folded α-Synuclein—To compare unfolded and folded α-synuclein, we acquired ^{1}H-^{15}N HSQC spectra of α-synuclein alone, or of α-synuclein in the presence of either SUVs (30% brain phosphatidylserine/70% phosphatidylcholine) or SDS (Fig. 4). The ^{1}H-^{15}N HSQC spectrum of α-synuclein alone exhibited a dense cluster of cross-peaks over a narrow range, confirming that the protein is unfolded as described previously (19). The number of visible peaks (~50) was less than expected (135), possibly because of aggregation or of fast chemical exchange between amide groups and the solvent. After addition of saturating concentrations of SUVs, many but not all of the α-synuclein cross-peaks disappeared. This loss of cross-peaks presumably occurred because the large size of the SUVs effectively broadened the resonances of the corresponding amide groups of α-synuclein beyond detection. The positions of α-synuclein cross-peaks that remained after binding to SUVs were unchanged from the spectrum of α-synuclein alone (Fig. 4*B*), showing that these cross-peaks represent amino acids that do not bind lipids and continue to be unfolded and mobile in the presence of SUVs. Consistent with previous results (19), we observed 36 such amino acids that account for a quarter of the total sequence.

The ^{1}H-^{15}N HSQC spectrum of α-synuclein obtained at saturating concentrations of SDS exhibited an increased dispersion compared with that of isolated α-synuclein (Fig. 4*C*). This result is consistent with the formation of α-helical structure upon micelle binding revealed by CD spectroscopy (Fig. 2). The number of visible cross-peaks also increased in SDS, most likely because SDS disrupts aggregation and/or because the formation of the α-helical conformation protected the amide groups from exchange with the solvent. Interestingly, the strongest cross-peaks observed in the presence of SDS were generally in the same positions as the cross-peaks that remained in the ^{1}H-^{15}N HSQC spectrum of α-synuclein bound to SUVs (Fig. 4*D*). Thus these cross-peaks correspond to unfolded residues that do not participate in binding to SDS micelles or to SUVs, supporting the notion that the binding modes and folding of α-synuclein in both environments are analogous.

Structural Analysis of Folded α-Synuclein—To study the structure of α-synuclein bound to SDS, we assigned its backbone signals using triple resonance and three-dimensional ^{1}H-^{15}N NOESY-HSQC and TOCSY-HSQC experiments (Fig. 5). Although a complete analysis of short range NOEs that are

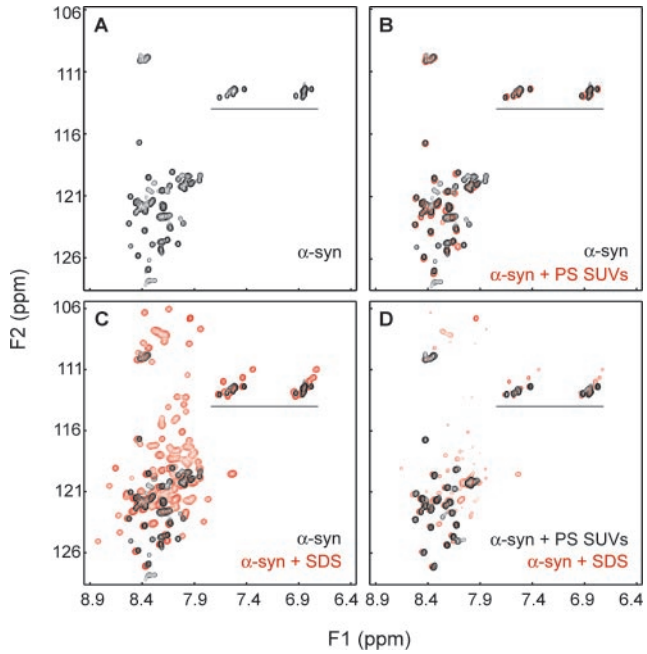

FIG. 4. **NMR Spectra of α-synuclein in the absence and presence of SUVs or SDS.** *A*, ^{1}H-^{15}N HSQC spectra of α-synuclein in 20 mM phosphate buffer, pH 7.4. *B*, overlay of the ^{1}H-^{15}N HSQC spectra of α-synuclein in the absence and presence of 30% brain phosphatidylserine, 70% phosphatidylcholine SUVs (0.1 mM α-synuclein with SUVs added at molar lipid to protein ratio of 280:1). Note the virtual superposition of the remaining peaks in the SUV spectrum with those of the α-synuclein spectrum. These represent amino acids that do not bind lipid and remain unfolded in the presence of SUVs. *C*, overlay of the spectra of α-synuclein in the absence and presence of SDS (20 mM). *D*, high level view of the spectra of α-synuclein in the presence of SUVs and SDS. Observe that most of the high intensity unfolded peaks in both spectra coincide. *Horizontal lines* in *A–D* indicate cross-peaks from Asn and Gln side chains.

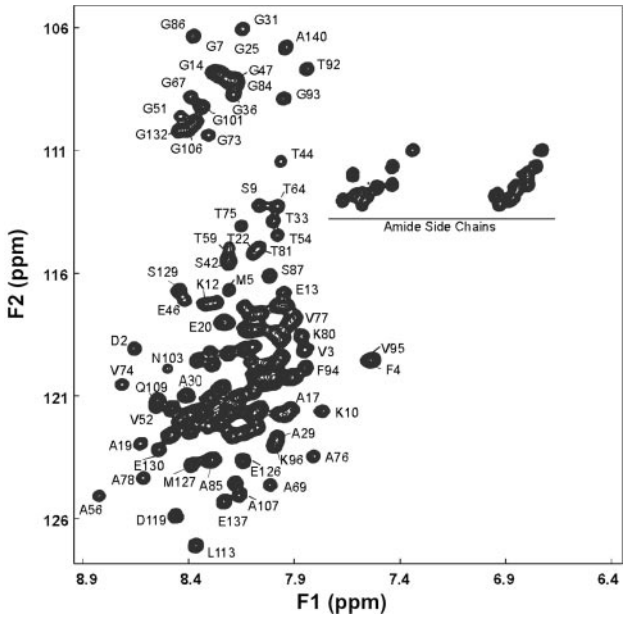

FIG. 5. **Backbone assignment of α-synuclein.** Assignment of cross-peaks in ^{1}H-^{15}N HSQC spectra of α-synuclein in the presence of SDS (0.3 mM α-synuclein in 50 mM SDS). Backbone signals were assigned using triple resonance and three-dimensional ^{1}H-^{15}N NOESY-HSQC and TOCSY-HSQC experiments. Resonance assignments have been deposited in the BioMagResBank under accession number 5744.

diagnostic for different types of secondary structure was made difficult by the strong resonance overlap observed, numerous NOEs could be assigned unambiguously. These include multi-

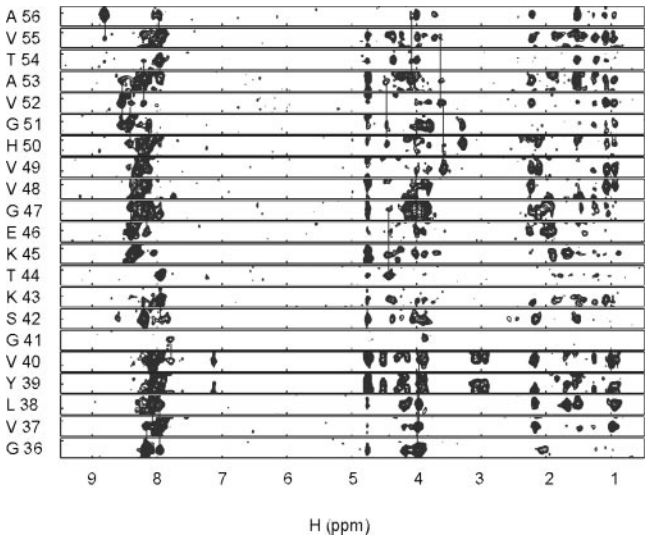

FIG. 6. **Composite of (F1, F3) strips of a three-dimensional ^{1}H-^{15}N NOESY-HSQC spectrum of SDS-bound α-synuclein illustrating the NOE patterns observed for residues 36–56.** *Solid lines* connect diagonal peaks with dNN(*i*,*i*+1) NOEs as well as intraresidue dαN(*i*,*i*) NOEs with dαN(*i*,*i*+3) connectivities.

ple NOEs that are characteristic of α-helical structure, particularly dNN(*i*,*i*+1) and dαN(*i*,*i*+3) NOEs, and are illustrated in sample strips from a three-dimensional ^{1}H-^{15}N NOESY-HSQC spectrum in Fig. 6. All dNN(*i*,*i*+1) and dαN(*i*,*i*+3) NOEs that could be assigned are summarized in Fig. 7 with *black boxes* and *solid lines*, respectively, whereas *open boxes* and *dashed lines* indicate dNN(*i*,*i*+1) and dαN(*i*,*i*+3) NOEs that could not be assessed because of resonance overlap. Note that dNN(*i*,*i*+1)/dαN(*i*,*i*+1) intensity ratios, rather than absolute dNN(*i*,*i*+1) intensities, are represented in Fig. 7 to account for differences in resonance line widths. Only a few dαN(*i*,*i*+2) and dαN(*i*,*i*+4) NOEs could be assigned unambiguously due to the resonance overlap and the limited sensitivity of the data obtained under the conditions of these experiments (data not shown).

The NOE data show that most of the 100 N-terminal residues, which include the seven 11-residue repeats, adopt an α-helical conformation. Interestingly, a noticeable break in the helical pattern was observed around residues 43 and 44, revealing an interruption of the helical structure in this region. This break in the helix was also apparent from analysis of the deviations of the observed Cα chemical shifts from random coil values (Fig. 8*A*). Significant positive deviations, which are characteristic of helical structure, were found for most of the N-terminal 98 residues, but the Cα chemical shifts of residues 43 and 44 were close to random coil values. The abundance of glycines in synuclein made analysis of Hα chemical shift deviations from random coil values difficult because the presence of two Hα protons in each glycine introduces uncertainty in the corresponding deviations. However, these data also illustrated the break in the helix (Fig. 8*B*). This conclusion is based on the negative deviations characteristic of helical structure that are observed for most of the 100 N-terminal residues, whereas residues 43–45 exhibit slightly positive deviations. In the sequences spanning residues 30–42, 60–65, and 82–100, a few Hα deviations are close to zero, and the Cα deviations are relatively small compared with other parts of the molecule, suggesting that there is helix fraying in these residues. However, the Cα deviations are still around 2 ppm or larger, and these sequences exhibit abundant dNN(*i*,*i*+1) and dαN(*i*,*i*+3) NOE patterns. Thus, these sequences adopt predominantly α-helical conformations that may be partially destabilized by the presence of residues with low helical propensity such as glycines and threonines.

The lack of sequential dNN(*i*,*i*+1) and short-range NOEs in the 40 C-terminal residues (Fig. 7) clearly shows that this region of the molecule is largely unstructured. This conclusion is further supported by the observation of sharper resonances in this region than in the rest of the molecule (illustrated by the ^{1}H-^{15}N HSQC cross-peaks; Fig. 4*D*) and by the small Cα and Hα deviations from random coil chemical shifts (Fig. 8; note that some significant deviations from random coil values may be favored by the abundance of prolines in this region). Extensive analysis of NOESY data did not uncover long-range NOEs indicative of tertiary structure, suggesting that the two α-helices do not interact with each other and are formed only at the protein/micelle interface. This conclusion agrees with the moderate chemical shift dispersion observed in SDS-bound α-synuclein, which indicates the presence of a defined secondary structure but is lower than the dispersion usually observed in globular proteins. Deuterium exchange experiments monitored at pH 6.5 by ^{1}H-^{15}N HSQC spectra further reinforced the conclusion that SDS-bound α-synuclein does not have a tertiary structure because all amide groups were largely exchanged with the solvent within the time scale of the first spectrum (30 min; data not shown).

To assess the secondary structure of α-synuclein by an independent approach, we examined the accessibility of each amino acid of α-synuclein to solvent by measuring their exchange cross-peaks with water using three-dimensional ^{15}N NOESY-HSQC and TOCSY-HSQC spectra (summarized in Fig. 7). The intensity of the exchange cross-peaks directly reflects the exposure of the respective amino acid to solvent. We observed strong exchange cross-peaks, which are indicative of a lack of amide protection for the unstructured C-terminal residues consistent with the non-structured nature of the corresponding sequence (see above). Furthermore, exchange cross-peaks were weak or absent for much of the residues in the helical regions as expected. In the region around residues 43–44, however, exchange cross-peaks with intermediate intensity were observed, which confirms the helical break in this region. Overall, the NMR data yield a picture whereby the 100 N-terminal residues of α-synuclein bound to SDS do not form a globular structure but adopt an α-helical conformation with a break in the middle.

The discovery of two α-helices in the folded conformation of α-synuclein was unanticipated as secondary structure calculations performed for example with the Expasy program suite (us.expasy.org) predict a mixture of α-helices, random coils, and β-strand. However, the NMR results correlate with the partial proteolysis experiments described above, which uncovered N-terminal protected 4 and 6 kDa bands that correspond to the first α-helix (Fig. 3). The observation of this proteolysis pattern in α-synuclein bound to both SUVs and SDS argues that their conformations are analogous.

Absence of Folding Intermediates—At non-saturating concentrations of SUVs or SDS, CD spectra of α-synuclein exhibited intermediate molar ellipticities (Fig. 1). Under these conditions, either only a subset of α-synuclein molecules was fully folded or a defined region of all synuclein molecules, such as part of an α-helix, was folded before the other regions. The first model implies that binding of both helical regions is a cooperative all-or-none process, whereas the second model would involve intermediate states containing partial helices. To distinguish between these possibilities, we acquired an ^{1}H-^{15}N HSQC spectrum of 0.1 mM synuclein at an intermediate SDS concentration (2.8 mM). If partially helical intermediates exist under these conditions, sharp cross-peaks in the positions cor-

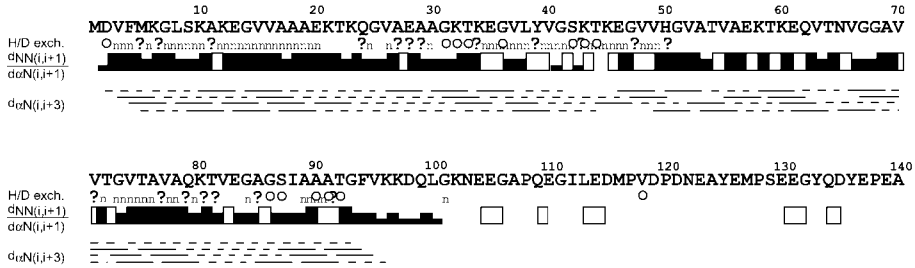

FIG. 7. **Secondary structure of α-synuclein bound to SDS micelles.** The primary sequence of α-synuclein is shown on *top*, and amide protection data and diagnostic NOE patterns are summarized *below* the sequence. Amide protection was assessed from the intensities of exchange cross-peaks with the solvent in three-dimensional ^{1}H-^{15}N NOESY-HSQC and TOCSY-HSQC spectra. The intensities were classified in three categories (weak, intermediate, and strong). Amide groups were considered protected from exchange if no cross-peak or a weak cross-peak with the solvent was observed (*closed circles*), whereas an intermediate exchange cross-peak intensity indicated partial protection (*open circles*). *Question marks* indicate amide groups whose protection could not be assessed due to resonance overlap. *Solid boxes* indicate the observation of dNN(i,i+1) NOEs. The height of the boxes reflects the intensity ratio between dNN(i,i+1) and dαN(i,i+1) connectivities, classified into three categories: >1, strong; 0.6–1, medium; <0.6, weak. *Open boxes* indicate dNN(i,i+1) connectivities that cannot be assessed due to resonance overlap. Observed dαN(i,i+3) NOEs are represented by *solid lines*, whereas *dashed lines* indicate dαN(i,i+3) NOES that could not be assessed because of resonance overlap.

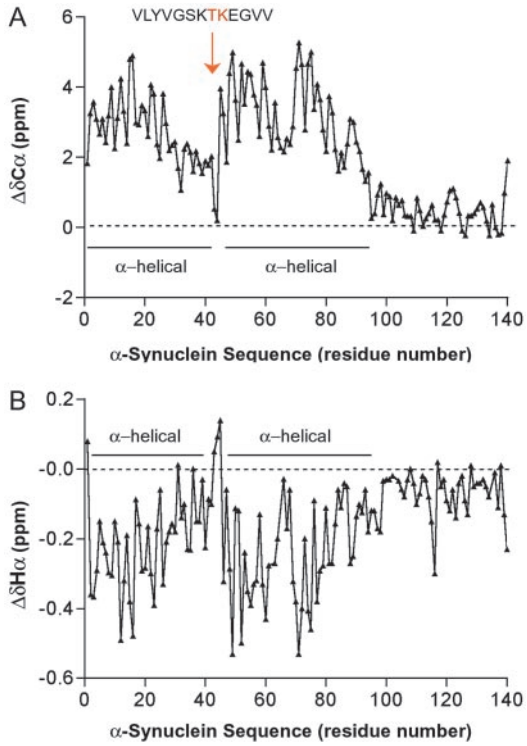

FIG. 8. **Conformational shifts of α-synuclein bound to SDS.** Plots of the differences between the Cα (*A*) and Hα (*B*) chemical shifts observed for α-synuclein in SDS and those expected for a random coil conformation as a function of the residue number. Helical regions are characterized by positive values for ΔδCα and negative values for ΔδHα. Random coil chemical shifts were obtained from the BioMagResBank. The *arrow* identifies the break in the α-helix at which the values for ΔδCα and ΔδHα resemble those of residues in a random coil conformation.

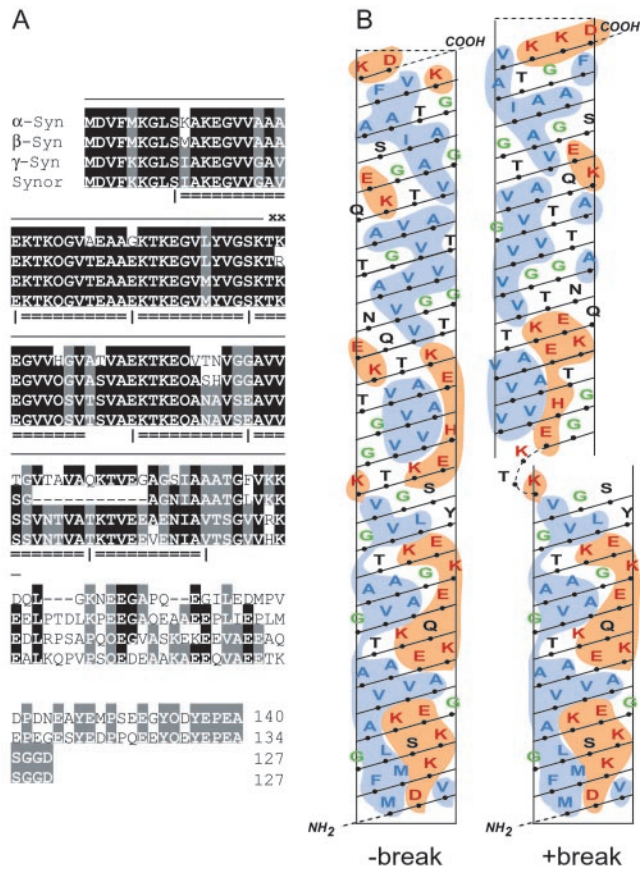

FIG. 9. **Primary and secondary structure of synucleins.** *A*, sequence alignment of human synucleins with identification of the eleven-residue repeats and the localization of α-helices. Residues shared among all synucleins are highlighted in *black*, whereas residues shared among two of the four synucleins are highlighted in *gray*. The two helices are indicated by *solid lines*, with the break being denoted by *xx*. The *hatched lines* below the alignment show the eleven-residue repeats. *B*, two-dimensional representation of the three-dimensional conformation of the N-terminal 98 residues of α-synuclein on a helical net. α-Synuclein is shown in a modeled conformation as a single continuous α-helix without a break (*left*) or in the observed conformation as two α-helices with a two-residue break (*right*). Hydrophobic residues are shown in *blue*, charged residues in *red*, and glycines in *green*. The N terminus with the initiating methionine is at the *bottom* and the C terminus on *top* as indicated.

responding to the unbound protein would be expected for the regions that remain unstructured. However, all of the cross-peaks corresponding to the two α-helices that could be identified were substantially broadened, and their positions were close to those observed for fully SDS-bound synuclein (data not shown). These results suggest that under these conditions, synuclein is in an equilibrium between free and fully bound states, although we cannot completely discard the possibility that the bound states are somewhat different from those existing at saturating SDS concentrations.

Implications for α-Synuclein Function and Dysfunction—We have shown that SUVs containing phosphatidylserine and SDS induce folding of α-synuclein in a concentration-dependent manner, with saturation at ~140 phospholipid or 70 SDS molecules per α-synuclein molecule. In folded α-synuclein, the

N-terminal 98 residues are structured, whereas the C-terminal 42 residues retain a random coil configuration. The structured part of α-synuclein forms two distinct α-helices that are interrupted by a two-residue break. Folding appears to be cooperative, without a stable intermediate at non-saturating concentrations of SDS or SUVs. In the folded state, no long-range interactions between α-synuclein residues were observed, suggesting that there is no tertiary structure and that all of the folded residues are directly or indirectly engaged in lipid binding.

The presence of two α-helices in α-synuclein and the position of the break were unexpected. α-Synuclein is composed of seven imperfect repeats composed of 11 residues. These repeats are interrupted after the fourth repeat by a four-residue insertion. The break between the two α-helices occurs in the first half of the fourth repeat, whereas the four-residue inserted sequence is α-helical. Furthermore, the break between the two α-helices consists of only two instead of four residues (Fig. 9*A*). Thus the break is not caused by the four-residue insertion between repeats; rather, the four-residue insertion serves to maintain the helical structure. When the two α-helices of α-synuclein are analyzed on a helical net, an amphipathic distribution of residues emerges, which explains the avid binding to negatively charged phospholipids (Fig. 9*B*). However, when the sequence of α-synuclein is modeled into a single α-helix without a break, the orientation of the hydrophobic surface shifts along the α-helix, suggesting that the break between the two helices may allow a more favorable binding of hydrophobic surfaces to the hydrophobic interior of the micelle/membrane. Binding is likely to be stabilized by ionic interactions between positive charged α-synuclein residues and negatively charged phospholipid headgroups because no α-helicity was observed with either membranes or detergents that do not contain negative surface charges. An alternative explanation for the break is that it may facilitate binding of α-synuclein to small vesicles with a high curvature such as synaptic vesicles. If uninterrupted, the α-helix of synuclein would measure 14 nm, which may be too long to coat a highly curved surface.

Our results suggest that α-synuclein may function as a surface-active coat of phospholipid membranes in the presynaptic nerve terminal, possibly of synaptic vesicles (20, 21). Indeed, tryptic digestion of α-synuclein in the presence of synaptic vesicles resulted in protection of N-terminal fragments similar to those seen with phosphatidylserine-containing SUVs (data not shown), indicating that α-synuclein binds to and folds on synaptic vesicles. Alignment of the four human synucleins shows that other synucleins probably adopt a similar secondary structure as α-synuclein (Fig. 9*A*). The sequences of the two α-helices and of the break are well conserved, whereas the non-folded C termini are not. However, α-synuclein is unique among synucleins because it has a longer second α-helix than β-synuclein, and a more hydrophobic surface than γ-synuclein or synoretin (Fig. 9*A*). These differences may explain the selective propensity of α-synuclein to aggregate in neurodegenerative diseases. Several recent studies (11–13) have shown that lipidic environments that promote α-synuclein folding also accelerate α-synuclein aggregation, suggesting that the lipid-associated conformation described here may be relevant to α-synuclein misfolding in neurodegenerative diseases.

Acknowledgments—We thank Dirk Fasshauer, Shigeo Takamori, and Wolfram Antonin for help and advice. We also thank Dietmar Riedel for analysis of SUVs by electron microscopy.

REFERENCES

1. Clayton, D. F., and George, J. M. (1998) *Trends Neurosci.* **21,** 249–254
2. Kahle, P. J., Neumann, M., Ozmen, L., and Haass, C. (2000) *Ann. N. Y. Acad. Sci.* **920,** 33–41
3. Goedert, M. (2001) *Nat. Rev. Neurosci.* **2,** 492–501
4. George, J. M., Jin, H., Woods, W. S., and Clayton, D. F. (1995) *Neuron* **15,** 361–372
5. Withers, G. S., George, J. M., Banker, G. A., and Clayton, D. F. (1997) *Brain Res. Dev. Brain Res.* **99,** 87–94
6. Ellis, C. E., Schwartzberg, P. L., Grider, T. L., Fink, D. W., and Nussbaum, R. L. (2001) *J. Biol. Chem.* **276,** 3879–3884
7. Maroteaux, L., and Scheller, R. H. (1991) *Brain Res. Mol. Brain Res.* **11,** 335–343
8. Akopian, A. N., and Wood, J. N. (1995) *J. Biol. Chem.* **270,** 21264–21270
9. Ji, H., Liu, Y. E., Jia, T., Wang, M., Liu, J., Xiao, G., Joseph, B. K., Rosen, C., and Shi, Y. E. (1997) *Cancer Res.* **57,** 759–764
10. Davidson, W. S., Jonas, A., Clayton, D. F., and George, J. M. (1998) *J. Biol. Chem.* **273,** 9443–9449
11. Conway, K. A., Harper, J. D., and Lansbury P. T., Jr. (2000) *Biochemistry* **39,** 2552–2563
12. Lee, H. J., Choi, C., and Lee S. J. (2002) *J. Biol. Chem.* **277,** 671–678
13. Narayanan, V., and Scarlata, S. (2001) *Biochemistry* **40,** 9927–9934
14. Schagger, H., and von Jagow, G. (1987) *Anal. Biochem.* **66,** 368–379
15. Muhandiram, D. R., and Kay, L. E. (1994) *J. Magn. Reson. B* **103,** 203–216
16. Zhang, O., Kay, L. E., Olivier, J. P., and Forman-Kay, J. (1994) *J. Biomol. NMR* **4,** 845–858
17. Barenholz, Y., Gibbes, D., Litman, B. J., Goll, J., Thompson, T. E., and Carlson, R. D. (1977) *Biochemistry* **16,** 2806–2810
18. Budavari, S. (1996) *The Merck Index: An Encyclopedia of Chemicals, Drugs and Biologicals*, 12th Ed., p. 8782, Whitehouse Station, NJ
19. Eliezer, D., Kutluay, E., Bussell, R., Jr., and Browne, G. (2001) *J. Mol. Biol.* **307,** 1061–1073
20. Jensen, P. H., Nielsen, M. S., Jakes, R., Dotti, C. G., and Goedert, M. (1998) *J. Biol. Chem.* **273,** 26292–26294
21. Kahle, P. J., Neumann, M., Ozmen, L., Muller, V., Jacobsen, H., Schindzielorz, A., Okochi, M., Leimer, U., van der Putten, H., Probst, A., Kremmer, E., Kretzschmar, H. A., and Haass, C. (2000) *J. Neurosci.* **20,** 6365–6373

PROTEIN STRUCTURE AND FOLDING:

A Broken α-Helix in Folded α-Synuclein

Sreeganga Chandra, Xiaocheng Chen, Josep Rizo, Reinhard Jahn and Thomas C. Südhof

J. Biol. Chem. 2003, 278:15313-15318.
doi: 10.1074/jbc.M213128200 originally published online February 13, 2003